Seasonally resolved growth of freshwater bivalves determined by oxygen and carbon isotope shell chemistry

Geochemistry Geophysics Geosystems G3

Article
Volume 11, Number 8
26 August 2010
Q08022, doi:10.1029/2009GC002961
ISSN: 1525-2027

Published by AGU and the Geochemical Society

Seasonally resolved growth of freshwater bivalves determined by oxygen and carbon isotope shell chemistry

Emma A. A. Versteegh, Hubert B. Vonhof, Simon R. Troelstra, and Ron J. G. Kaandorp
Institute of Earth Sciences, VU University Amsterdam, De Boelelaan 1085, NL-1081 HV Amsterdam, Netherlands (emma.versteegh@vub.ac.be)

Dick Kroon
School of GeoSciences, University of Edinburgh, West Mains Road, Edinburgh EH9 3JW, UK

[1] By means of a monitoring experiment in two rivers in the Netherlands, we establish a relationship between seasonally resolved growth rates in unionid freshwater bivalves and their environment. We reconstructed these seasonally resolved growth rates by using relationships of stable isotopes in the shells and their ambient river water. The reconstructed growth rates reveal that shells grow fastest in spring-early summer, when highest food availability occurs in the rivers. In addition, the reconstructed growth rates show that onset and cessation of growth are mainly influenced by water temperature.

Components: 7100 words, 11 figures, 2 tables.

Keywords: Bivalvia; Meuse; Rhine; seasonality; *Unio*; Unionidae.

Index Terms: 0454 Biogeosciences: Isotopic composition and chemistry (1041); 0473 Biogeosciences: Paleoclimatology and paleoceanography (3344); 1041 Geochemistry: Stable isotope geochemistry (0454).

Received 16 November 2009; **Revised** 23 June 2010; **Accepted** 1 July 2010; **Published** 26 August 2010.

Versteegh, E. A. A., H. B. Vonhof, S. R. Troelstra, R. J. G. Kaandorp, and D. Kroon (2010), Seasonally resolved growth of freshwater bivalves determined by oxygen and carbon isotope shell chemistry, *Geochem. Geophys. Geosyst.*, *11*, Q08022, doi:10.1029/2009GC002961.

1. Introduction

[2] Ontogenetic growth rate patterns of unionid freshwater mussels have been described by a number of authors [*Anthony et al.*, 2001; *Morris and Corkum*, 1999; *Versteegh et al.*, 2009] and are inferred to be influenced by several factors including but not limited to: temperature [*Dettman et al.*, 1999; *Goodwin et al.*, 2003]; turbidity; nutrient availability and primary productivity [*Arter*, 1989; *Kesler et al.*, 2007; *Valdovinos and Pedreros*, 2007]. With respect to intraannual growth *Dunca and Mutvei* [2001] and *Dunca et al.* [2005] found that daily growth lines have a strong positive relationship with temperature in *Margaritifera margaritifera*. However, information on unionid intraannual growth remains relatively sparse [*Howard*, 1922; *Negus*, 1966].

[3] In order to understand the environmental signals influencing growth rates, it is essential to document the influence of environmental factors on intraannual growth rates in monitoring experiments. In this study, we present such a monitoring experiment investigating three unionid species that

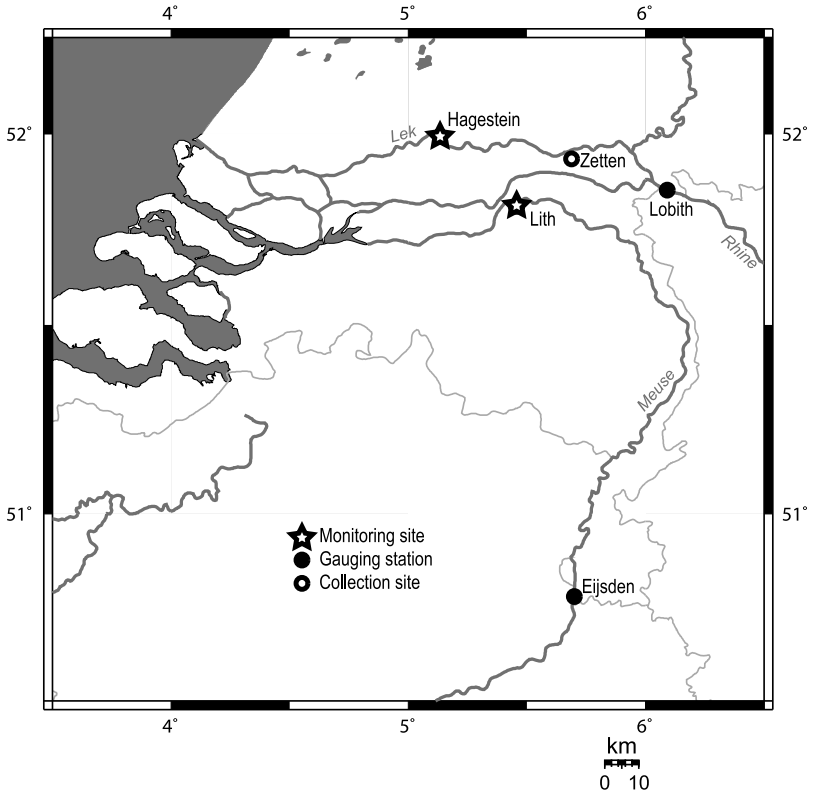

Figure 1. Map of part of the Dutch Rhine-Meuse delta with shell collection site at Zetten, monitoring sites at Hagestein and Lith and Rijkswaterstaat gauging stations at Eijsden and Lobith (made with online map creation, http://www.aquarius.geomar.de/).

naturally occur in the Meuse and Rhine (The Netherlands): *Anodonta anatina*, *Unio pictorum* and *U. tumidus*.

[4] We aim to investigate the relationship between the stable isotopic composition of shell growth increments and seasonal changes in river water composition. Using this relationship the intraannual growth rates of individual shells can be determined allowing for a better understanding of which environmental factors dominate seasonal growth rate variability.

2. Materials and Methods

2.1. Monitoring

[5] Unionid freshwater mussels are abundant in the Dutch part of the Rhine-Meuse delta. They can reach an age of approximately 15 years and sizes up to 13 cm. [*Gittenberger et al.*, 1998]. For this study, monitoring sites were established in fish ladders near weirs in the rivers Meuse and Lek (a Rhine distributary) in the Netherlands. These sites were selected for the relatively constant water levels and flow velocities. The Meuse weir is situated near Lith, the Lek weir at Hagestein (Figure 1).

[6] From the River Linge at Zetten (Figure 1) seven living specimens (three adult *Unio pictorum*, three adult *U. tumidus* and one juvenile *Anodonta anatina*) were collected on 26 January 2006. The specimens were tagged using 8 × 4 mm Hallprint type FPN glue-on shellfish tags with cyanoacrylate adhesive (standard 'Superglue', following the methodology of *Lemarié et al.* [2000] and *Ross et al.* [2001]) and were then placed in a cage at the Hagestein monitoring station. The cage design has been described by *Versteegh* [2009] and consists of a 22 × 40 × 60 cm PVC box with a 5 cm perforated stainless steel top. At the Lith monitoring station four living mussels of the species *U. pictorum* acquired from a pet shop were placed into a similar cage on 6 July 2006. During winter two specimens were collected at both sites (Table 1) and killed by freezing. The experiment was concluded at both sites by freezing the mussels on 12 July 2007. Specifications of the specimens are given in Table 1.

Table 1. Specifications of Shell Samples

	Species	Length (mm)	Height (mm)	Height Along Shell (mm)	Collection Site	Monitoring Site	Start Date	End Date
3110	*Unio tumidus*	78.8	38.2	54	Linge; Zetten	Hagestein	26-Jan-06	5-Apr-07
3114	*Unio pictorum*	63.5	27.2	39	Linge; Zetten	Hagestein	26-Jan-06	12-Jul-07
3115	*Unio pictorum*	86.6	36.9	50	Linge; Zetten	Hagestein	26-Jan-06	12-Jul-07
3117	*Unio pictorum*	61.2	26.7	39	Linge; Zetten	Hagestein	26-Jan-06	5-Apr-07
3119	*Unio tumidus*	45.0	24.0	34	Linge; Zetten	Hagestein	26-Jan-06	12-Jul-07
3129	*Unio tumidus*	64.4	32.4	43	Linge; Zetten	Hagestein	26-Jan-06	12-Jul-07
3135	*Anodonta anatina*	35.0	19.3	25	Linge; Zetten	Hagestein	26-Jan-06	12-Jul-07
3149	*Unio pictorum*	75.3	30.4	43	Pet shop	Lith	6-Jul-06	14-Dec-06
3153	*Unio pictorum*	81.8	33.2	47	Pet shop	Lith	6-Jul-06	14-Dec-06
3170	*Unio pictorum*	77.1	31.9	44	Pet shop	Lith	6-Jul-06	12-Jul-07
3172	*Unio pictorum*	69.8	29.9	44	Pet shop	Lith	6-Jul-06	12-Jul-07

[7] Water samples for isotope analysis were taken biweekly for a period of 18 months at Hagestein and a period of 12 months at Lith. The 100 ml samples were conserved with two drops of a solution of 15 mg of I_2 and 30 mg of KI per ml of milliQ water [*Mook*, 2000]. Water temperature was logged with an ATAL ATX-01E temperature data recorder in a waterproof container at hourly intervals.

[8] Additional water oxygen isotope ($\delta^{18}O_w$) data of both rivers, covering the years 2006 and 2007 and measured at Eijsden and Lobith (Figure 1), were obtained from the Centre for Isotope Research (University of Groningen).

[9] Biweekly recorded data on pH and chlorophyll *a* (a measure of primary productivity) in the water were obtained from Rijkswaterstaat (Dutch Directorate for Public Works and Water Management) at Eijsden (Meuse) and Lobith (Rhine) (Figure 1).

2.2. Analyses

[10] All shells were measured with respect to their length and height (Table 1) and then embedded in epoxy resin. Sections of 300 μm thickness were cut perpendicular to the growth lines, along the dorsoventral axis and through the umbo [*Versteegh et al.*, 2009]. The nacreous layer of the shells was sampled with a Merchantek Micromill micro sampler equipped with a ~ 800 μm drill bit by milling along the growth lines [*Versteegh*, 2009]. Considering the amount of carbonate between 10 and 50 μg required for mass spectrometry, the highest possible sampling resolution was chosen. The sampling distance varied between 30 and 200 μm with a Drilling depth of ~ 250 μm.

[11] Both shell and water samples were analyzed for oxygen and carbon isotope ratios ($\delta^{18}O$ and $\delta^{13}C$ values) using a Thermo Finnigan Delta+ mass spectrometer equipped with a GasBench-II preparation device. The long-term standard deviation of a routinely analyzed in-house $CaCO_3$ standard is < 0.1 ‰ for $\delta^{18}O$ values and < 0.09 for $\delta^{13}C$ values. This $CaCO_3$ standard is regularly calibrated to NBS 18, 19 and 20. The long-term standard deviation of a routinely analyzed in-house water standard is < 0.1 ‰ for $\delta^{18}O_w$ and is < 0.15 ‰ for $\delta^{13}C_{DIC}$ values, respectively.

2.3. Calculation of Predicted $\delta^{18}O_{ar}$ Values and Comparison With Measured $\delta^{18}O_{ar}$ Values

[12] Measured temperature and $\delta^{18}O_w$ values of ambient river water were used to calculate predicted $\delta^{18}O$ ($\delta^{18}O_{ar}$) values of shell aragonite precipitated in equilibrium, using the equation of *Grossman and Ku* [1986] in the form suggested by *Dettman et al.* [1999]:

$$1000\ln\alpha = 2.559(10^6T^{-2}) + 0.715 \quad (1)$$

where T is the water temperature in degrees Kelvin and α is the fractionation between water and aragonite.

[13] All oxygen isotope values are calculated relative to Vienna Standard Mean Ocean Water (VSMOW). $\delta^{18}O_{ar}$ values are, however, usually expressed relative to Vienna Pee Dee Belemnite (VPDB). To convert $\delta^{18}O_{ar}$ (VSMOW) values to $\delta^{18}O_{ar}$ (VPDB) values, the following equation has been used [*Gonfiantini et al.*, 1995]:

$$\delta^{18}O_{ar}(\text{VSMOW}) = 1.03091(1000 + \delta^{18}O_{ar}(\text{VPDB})) - 1000 \quad (2)$$

2.4. Calculation of Bicarbonate $\delta^{13}C$ Values and the Fractionation With Aragonite

[14] Measured river water pH values for both rivers ranged between 7.4 and 8.4, indicating

dissolved inorganic carbon (DIC) consisted mainly of HCO_3^- (bicarbonate) and low concentrations of H_2CO_3 and CO_3^{2-}. The relative concentrations of individual carbonate species, including H_2CO_3 HCO_3^- and CO_3^{2-} are obtained using the equations described by *Clark and Fritz* [1997] and *Zeebe and Wolf-Gladrow* [2001].

[15] While the isotopic fractionation of dissolved CO_2 relative to HCO_3^- is given by the following equation [*Mook*, 2000]:

$$\varepsilon_{H_2CO_3/HCO_3^-} = \frac{-9866}{T_K} + 24.12‰ \quad (3)$$

[16] Bicarbonate $\delta^{13}C$ values ($\delta^{13}C_{HCO3-}$) are calculated using the ratio H_2CO_3 / HCO_3^- and the fractionation between them. Isotopic enrichment factors between shell aragonite and HCO_3^- are calculated using the relation [*Romanek et al.*, 1992]:

$$\varepsilon_{ar/HCO_3^-} = 1000 \cdot \left[\left(\delta^{13}C_{ar} + 1000\right) \Big/ \left(\delta^{13}C_{HCO_3^-} + 1000\right) - 1\right] \quad (4)$$

[17] For inorganic precipitation of aragonite $\varepsilon_{ar/HCO3-}$ is 2.7 ± 0.6 ‰ [*Romanek et al.*, 1992]. However, in the biogenic aragonite of Peruvian unionids, a depletion of 4.0 ± 0.7 ‰ has been found by certain studies [*Kaandorp et al.*, 2003].

2.5. Construction of Seasonally Resolved Growth Models

[18] In order to accurately predict growth rates, four seasonally resolved models based on the isotopic compositions of shells and ambient water, were generated: (1) a linear model; (2) a model based upon predicted and observed seasonal $\delta^{18}O_{ar}$ records; (3) a model based upon the comparison of seasonal $\delta^{13}C_{HCO3-}$ and aragonite $\delta^{13}C$ ($\delta^{13}C_{ar}$) records, and (4) a model combining predicted and observed $\delta^{18}O_{ar}$ records as well as $\delta^{13}C_{HCO3-}$ and $\delta^{13}C_{ar}$ records.

[19] As a first step toward comparison of the measured and predicted $\delta^{18}O_{ar}$ records we start by assuming linear growth between the previously determined spring and autumn dates of onset and cessation of growth (model 1).

[20] To better understand the environmental factors driving seasonal growth rate changes we subsequently attempt to construct an improved seasonally resolved growth rate model based on peak matching (model 2). If $\delta^{18}O_{ar}$ values are in equilibrium with the ambient water we are not limited to correlating the first and last samples of the measured $\delta^{18}O_{ar}$ summer segments with the predicted $\delta^{18}O_{ar}$ profiles, but too all samples of each complete summer segment. First order correlation is based upon peaks and troughs in the records and then the remaining measured $\delta^{18}O_{ar}$ values between the peaks and troughs are shifted along the time axis to the closest values on the predicted $\delta^{18}O_{ar}$ graph [*Freitas et al.*, 2006]. If $\delta^{13}C_{ar}$ values do reflect $\delta^{13}C_{HCO3-}$ values a similar approach will be applied for stable carbon isotopes (model 3). The final seasonal growth model (4) attempts to simultaneously match peaks in both the $\delta^{13}C$ and $\delta^{18}O$ records.

3. Results

3.1. River Water

[21] While water temperatures in both locations varied seasonally with summer temperatures rising to about 25°C and winter values as low as 2°C (Figures 2a and 2b), no discernable patterns were observed in the pH values of either river. In the Lek the pH varied between 7.5 and 8.4 and in the Meuse between 7.4 and 8.2.

[22] During the monitoring period the $\delta^{18}O_w$ values varied between −9.8 and −7.9 ‰ (VSMOW) in the Lek and between −8.1 and −6.4 ‰ (VSMOW) in the Meuse. The average was −8.9 ‰ in the Lek while in the Meuse −7.1 ‰ (Figures 2a and 2b). The $\delta^{18}O_w$ data during the period of monitoring generally correspond with the data set from the Centre for Isotope Research (University of Groningen), plotted in Figures 2a and 2b.

[23] The $\delta^{13}C_{HCO3-}$ values measured (expressed in VPDB) range between −13.6 and −7.9 ‰ in the Lek and −15.3 and −8.6 ‰ in the Meuse (Figures 3a and 3b; due to the pH range of these rivers, the difference between $\delta^{13}C_{HCO3-}$ and $\delta^{13}C_{DIC}$ is negligible). Chlorophyll *a* concentrations exhibit seasonal patterns with 'background' values of 2 μg/l in both rivers with peaks occurring in late spring-early summer, up to 39 μg/l in the Lek and 56 μg/l in the Meuse, respectively (Figures 3a and 3b).

3.2. Shell Growth and Isotopic Composition

[24] Experimental commencement can be recognized as a growth disturbance line in a transverse section of the shell (Figure 4) due to the stress of

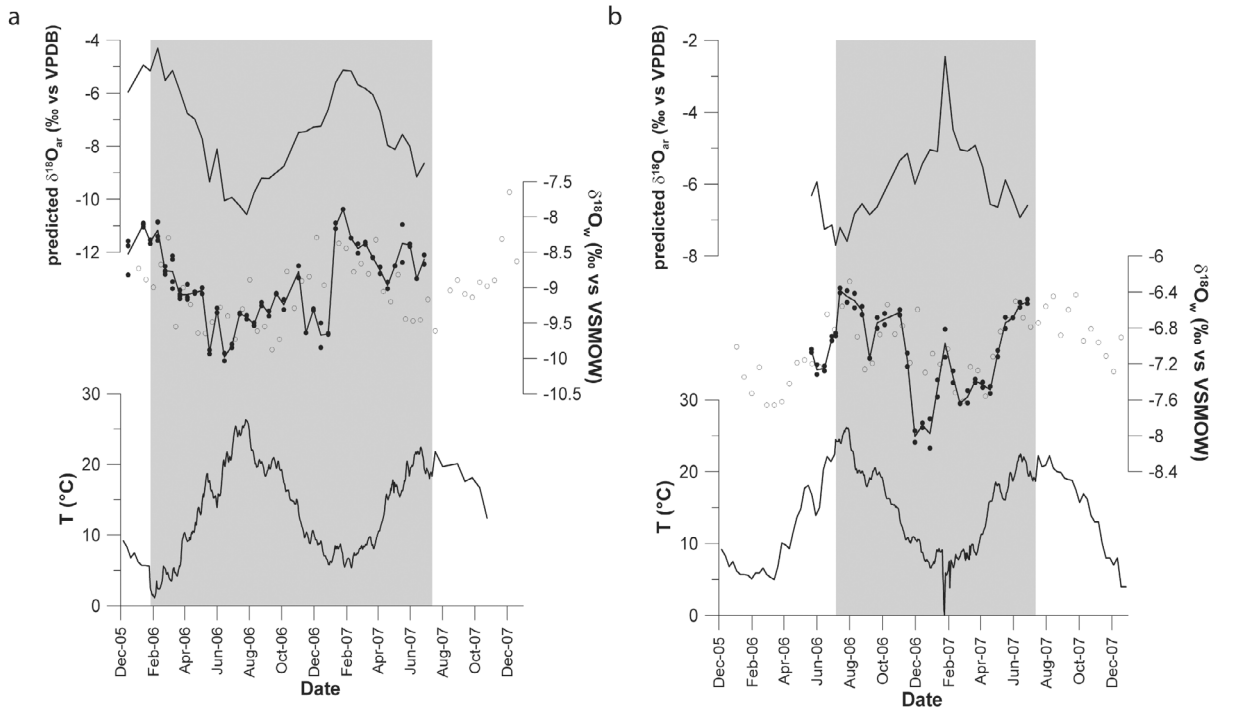

Figure 2. Water temperature (bottom line), $\delta^{18}O_w$ values (middle line) and resulting predicted $\delta^{18}O_{ar}$ values (top line) in 2006 and 2007: (a) in the river Lek and (b) in the Meuse. For $\delta^{18}O_w$ values both our own data set (black dots and solid line) and a data set from the Centre for Isotope Research, University of Groningen (open circles) are shown. Only our own data set is used for calculation of predicted $\delta^{18}O_{ar}$ values. Shaded in gray is the duration of the monitoring experiment for both locations.

collection or staining with calcein [*Clark*, 2005]. Using this as a correlative marker between co-habiting individuals estimates of the shell growth and $\delta^{18}O_{ar}$ values could be obtained. During the period of investigation individual shell growth varied between 0.1 and 3.4 mm, while $\delta^{18}O_{ar}$ values of the shells varied between −5.2 and −10.8 ‰ (average −8.9 ‰) in the river Lek (Figures 5a–5g), and between −6.1 and −6.8 ‰ (average −6.5 ‰) for the Meuse. Specimens from Lith grew too slowly to resolve any seasonal variations during the monitoring experiment, and these shells were therefore excluded from further analysis.

[25] With a single exception, the Hagestein shells demonstrated a seasonal pattern: a broad trough in summer and a narrow peak in winter together representing one year of growth [*Versteegh et al.*, 2009].

[26] The range of $\delta^{13}C_{ar}$ values for the same period is −9.1 to −14.2 ‰ in the Lek (Figures 5a–5g) and −11.2 to −13.3 ‰ in the Meuse. In the Meuse shells there are no detectable seasonal patterns in $\delta^{13}C_{ar}$ values, however with a singular exception (shell 3135, justifiable due to the low sampling resolution) a seasonal pattern in $\delta^{13}C_{ar}$ can be observed in the samples from the river Lek.

4. Discussion

4.1. Seasonal Isotope Variation of River Water

[27] $\delta^{18}O_w$ values of the Meuse and Rhine are known to display a seasonal cycle (Data: Centre for Isotope Research, University of Groningen, published by *Versteegh et al.* [2009]) owing to the seasonal variation in amount and composition of different source waters. The $\delta^{18}O_w$ value of the Meuse is determined by the relative contributions of groundwater and surface runoff. In winter, when evaporation is limited, $\delta^{18}O_w$ values reflect those of groundwater, whereas in summer $\delta^{18}O_w$ values are higher due to evaporation and enriched summer precipitation [*Mook*, 1968].

[28] In spring and early summer, the Rhine river system $\delta^{18}O_w$ values become isotopically depleted due to the influx of meltwater from the Alps. This meltwater and the inland location of the Rhine basin

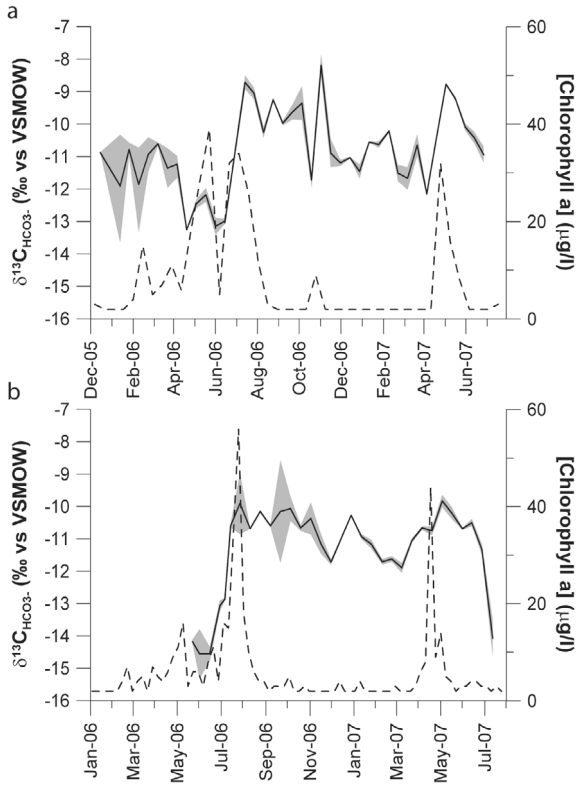

Figure 3. The $\delta^{13}C_{HCO3-}$ values (solid line) and chlorophyll *a* concentration (dashed line) during the monitoring experiment: (a) for the Lek at Hagestein and (b) for the Meuse at Lith. The gray area indicates the range of samples measured in duplicate.

on the European continent result in overall lower $\delta^{18}O_w$ ratios than those of the Meuse with lowest values in summer and highest values in winter [*Mook*, 1968; *Ricken et al.*, 2003; *Versteegh et al.*, 2009]. Thus, the Rhine and Meuse exhibit opposing seasonal $\delta^{18}O_w$ cycles (Figures 2a and 2b).

[29] With respect to $\delta^{13}C_{HCO3-}$ values, previous observations depicted both rivers to have seasonal patterns, with values ranging from −12.5 to −7.7 ‰ (Figure 6) with low values in winter and high values in summer [*Mook*, 1968, 2000]. Higher values in summer were ascribed to isotopic exchange with atmospheric CO_2 [*Mook and Vogel*, 1968].

[30] A similar seasonal pattern in $\delta^{13}C_{HCO3-}$ values was observed for both rivers during the period of study. Generally low $\delta^{13}C_{HCO3-}$ values occurred in winter and spring and high $\delta^{13}C_{HCO3-}$ values occurred in summer. However, the shifts toward positive values occurred rather abruptly, suggesting that a mechanism other than the proposed enhancement of carbon isotopic exchange with atmospheric CO_2 during summer months, is a reason for seasonality within $\delta^{13}C_{HCO3}$values [*Mook and Vogel*, 1968]. For instance, metabolic effects, like those of photosynthesis and respiration, are expected to have a profound influence on both ambient water $\delta^{13}C_{HCO3-}$ values and shell $\delta^{13}C_{ar}$ values [*McConnaughey et al.*, 1997; *McConnaughey and Gillikin*, 2008]. Photosynthesis by phytoplankton preferentially removes ^{12}C from the DIC pool [*Al-Aasm et al.*, 1998; *Fritz and Poplawski*, 1974], increasing $\delta^{13}C_{ar}$ values of shell aragonite precipitated from DIC. At the same time, phytoplankton, having very low $\delta^{13}C$ values, forms an important component of the unionid diet [*Nichols and Garling*, 2000; *Raikow and Hamilton*, 2001]. Algal and microbial carbon have been shown to conceivably lower shell $\delta^{13}C_{ar}$ values, depending on the level of metabolic carbon that has been incorporated [*McConnaughey and Gillikin*, 2008]. In order to investigate a possible relationship between $\delta^{13}C_{HCO3-}$ values and primary productivity, a time series of chlorophyll *a* concentrations representing phytoplankton abundance and thus primary productivity was compared with measured $\delta^{13}C_{HCO3-}$ values in Figures 3a and 3b. Sharp rises in $\delta^{13}C_{HCO3-}$ values can be seen to track peaks in chlorophyll *a* at both rivers, albeit with a less abrupt rise in the Meuse

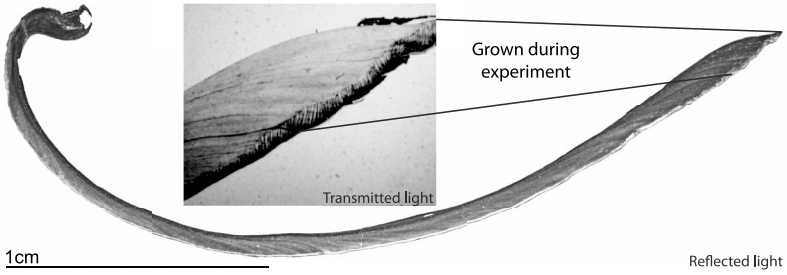

Figure 4. Transverse section through shell 3114 (*Unio pictorum*), photographed under reflected light, with a blow-up in transmitted light of the part of the shell grown during the monitoring experiment.

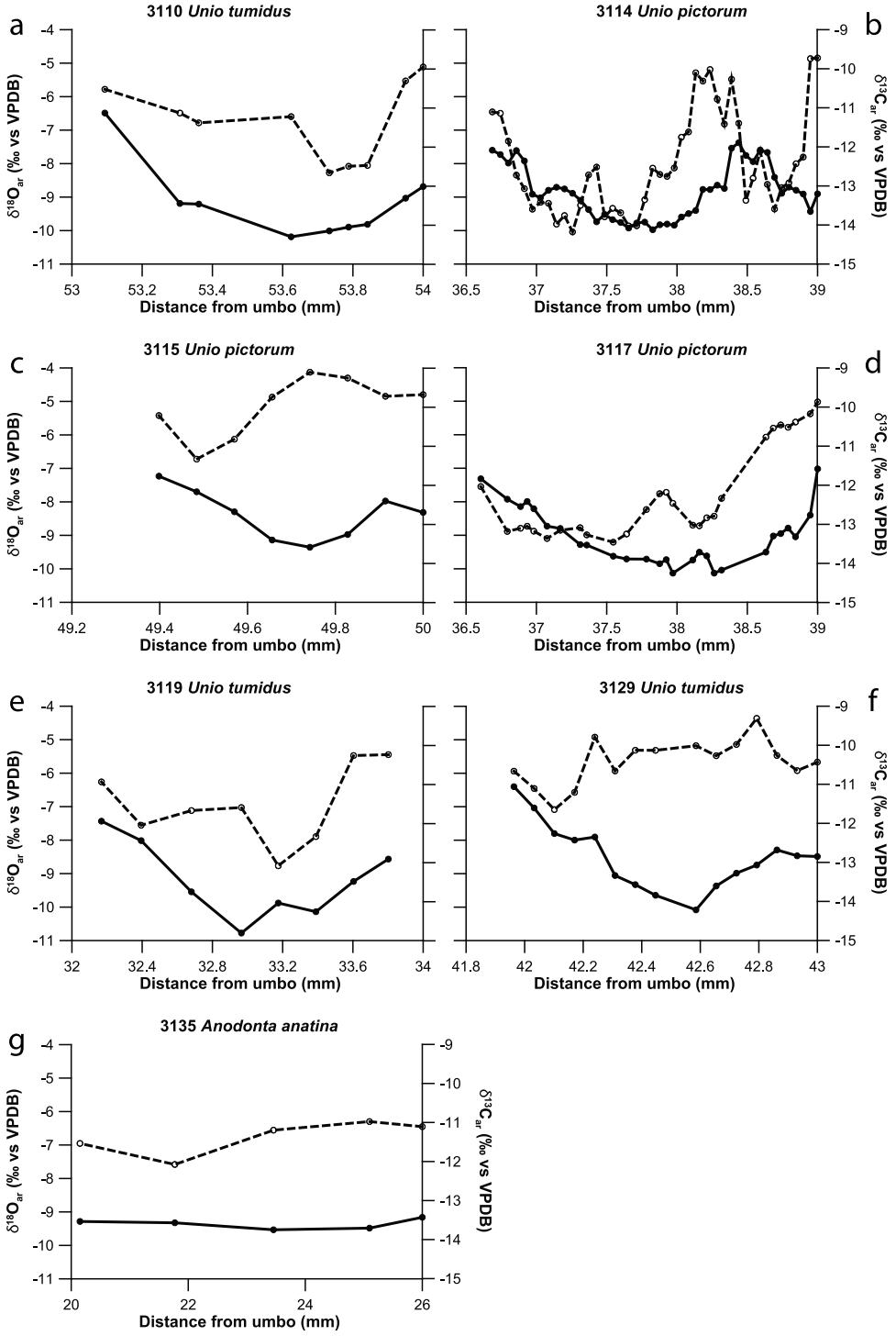

Figure 5. The $\delta^{18}O_{ar}$ values (solid lines and symbols) and $\delta^{13}C_{ar}$ values (dashed lines and open symbols) of the seven shells grown in Hagestein. The experiment covered the time interval January 2006–April 2007 in shells 3110 (Figure 5a) and 3117 (Figure 5d) and January 2006–July 2007 in the other shells.

than in the Lek during 2007. We therefore ascribe these rises in $\delta^{13}C_{HCO3-}$ values to preferential removal of ^{12}C by phytoplankton photosynthesis (Figures 3a and 3b).

4.2. Equilibrium Precipitation of Shell Aragonite: Oxygen Isotopes

[31] Unionid freshwater mussels can record characteristics of ambient water chemistry in their

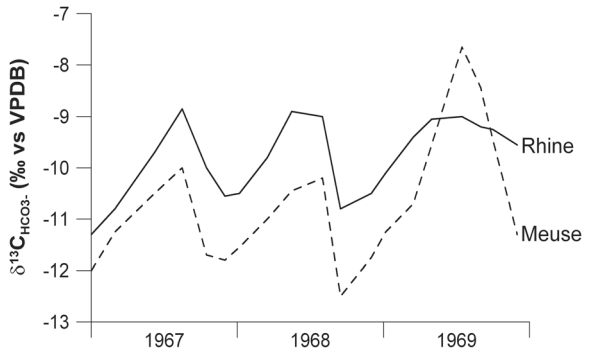

Figure 6. The $\delta^{13}C_{HCO3-}$ values for the Rhine and Meuse during the years 1967–1969 (data: W. G. Mook).

growth increments at high temporal resolution [*Ricken et al.*, 2003; *Verdegaal et al.*, 2005; *Versteegh et al.*, 2009, 2010]. $\delta^{18}O_{ar}$ values are generally found to be in equilibrium with ambient water [*Dettman et al.*, 1999; *Gajurel et al.*, 2006; *Goewert et al.*, 2007; *Kaandorp et al.*, 2003]. We investigated whether the two *Unio* species precipitated their shell in oxygen isotopic equilibrium with ambient water during the monitoring experiments, using $\delta^{18}O_w$ values and water temperature to predict $\delta^{18}O_{ar}$ values (equations (1)–(2) and Figures 2a and 2b). The sharp trough to 0°C in the Meuse water temperatures, and corresponding peak in predicted $\delta^{18}O_{ar}$ values (Figure 2b) is due to accidental exposure of the top of the cage, containing the temperature logger, caused by low water level in the fish ladder. However, since the mussels do not grow in winter, this is of no consequence for this study [*Anthony et al.*, 2001; *Goewert et al.*, 2007; *Kesler et al.*, 2007; *Versteegh et al.*, 2009].

[32] The measured $\delta^{18}O_{ar}$ values of the ventral margin of those specimens that both survived and continued to precipitate aragonite until the end of the experiment (shells 3114; 3115 and 3129; Figures 7b, 7c, and 7f, respectively) match the predicted values for the experimental end-date (Table 2). Shells 3119 and 3135 were observed to be still alive at the conclusion of the experiment, however curiously failed to precipitate any aragonite during the spring of 2007.

[33] While, the mussels were harvested on 12 July 2007 the isotopic measurements of the water from that date were unable to be retrieved and therefore samples taken on 27 June 2007 were used. This poses no problem for analytical reliability since the amount of time averaging within one ventral margin sample is about one week in shell 3114, but many weeks in shell 3115 and 3129. This latter fact is also the most likely cause for the deviations of up to 0.32 ‰ from predictions. These deviations are, however, small and not in a specific direction, confirming that aragonite is precipitated in oxygen isotopic equilibrium with ambient water.

4.3. Seasonal Shell Oxygen Isotope Records

[34] The measured $\delta^{18}O_{ar}$ records typically show a truncated sinusoidal pattern (e.g., Figure 5b), caused by a combination of temperature fractionation and seasonal growth cessation [*Dettman et al.*, 1999; *Goodwin et al.*, 2003; *Grossman and Ku*, 1986]. Since the shells did not grow in winter, $\delta^{18}O_{ar}$ records contain (invisible) gaps resulting in juxtaposed increments of (summer) shell growth.

[35] The fact that aragonite is precipitated in oxygen isotopic equilibrium with ambient water enables us to compare predicted and measured $\delta^{18}O_{ar}$ records and subsequently determine the temperature of seasonal growth initiation and cessation. Alignment of measured $\delta^{18}O_{ar}$ summer segments with the predicted $\delta^{18}O_{ar}$ record documented that shell growth initiated above 13.5 ± 2.8°C and ceased below 13.5 ± 4.2°C. This corresponds to values previously observed [*Negus*, 1966].

4.4. Shell Carbon Isotope Records

[36] While $\delta^{13}C$ values of mollusk shells have yielded a plethora of practical environmental information, many questions relating to the processes behind trends in seasonal shell $\delta^{13}C$ records remain unanswered. Despite the fact that several authors have reported covariation between $\delta^{13}C$ values in bivalves and those of DIC [*Aucour et al.*, 2003; *Buhl et al.*, 1991; *Fritz and Poplawski*, 1974; *Kaandorp et al.*, 2003], others have failed to reproduce these results. This failure to detect any relationship between shell $\delta^{13}C$ and $\delta^{13}C_{DIC}$ is usually ascribed to the incorporation of metabolic carbon into the shell [*Fastovsky et al.*, 1993; *Gajurel et al.*, 2006; *Geist et al.*, 2005; *Ricken et al.*, 2003; *Veinott and Cornett*, 1998; *Verdegaal et al.*, 2005]. However, *Gillikin et al.* [2009] suggest that an ontogenetic increase in metabolic carbon does not exclude $\delta^{13}C$ data of unionid freshwater mussels from being a useful environmental proxy. Detection of a relationship between $\delta^{13}C_{ar}$ and $\delta^{13}C_{DIC}$ in previous studies may have been hampered by uncertainties in time correlation of isotope records in water with those in shells [*Dettman et al.*, 1999].

[37] The observed shifts in the $\delta^{13}C_{HCO3-}$ records are sufficiently large (> 2 ‰) to be recorded in bivalve shells [*Gillikin et al.*, 2006]. This indeed appears to be the case: with the exceptions of shells with low sampling resolution, shell 3135 from

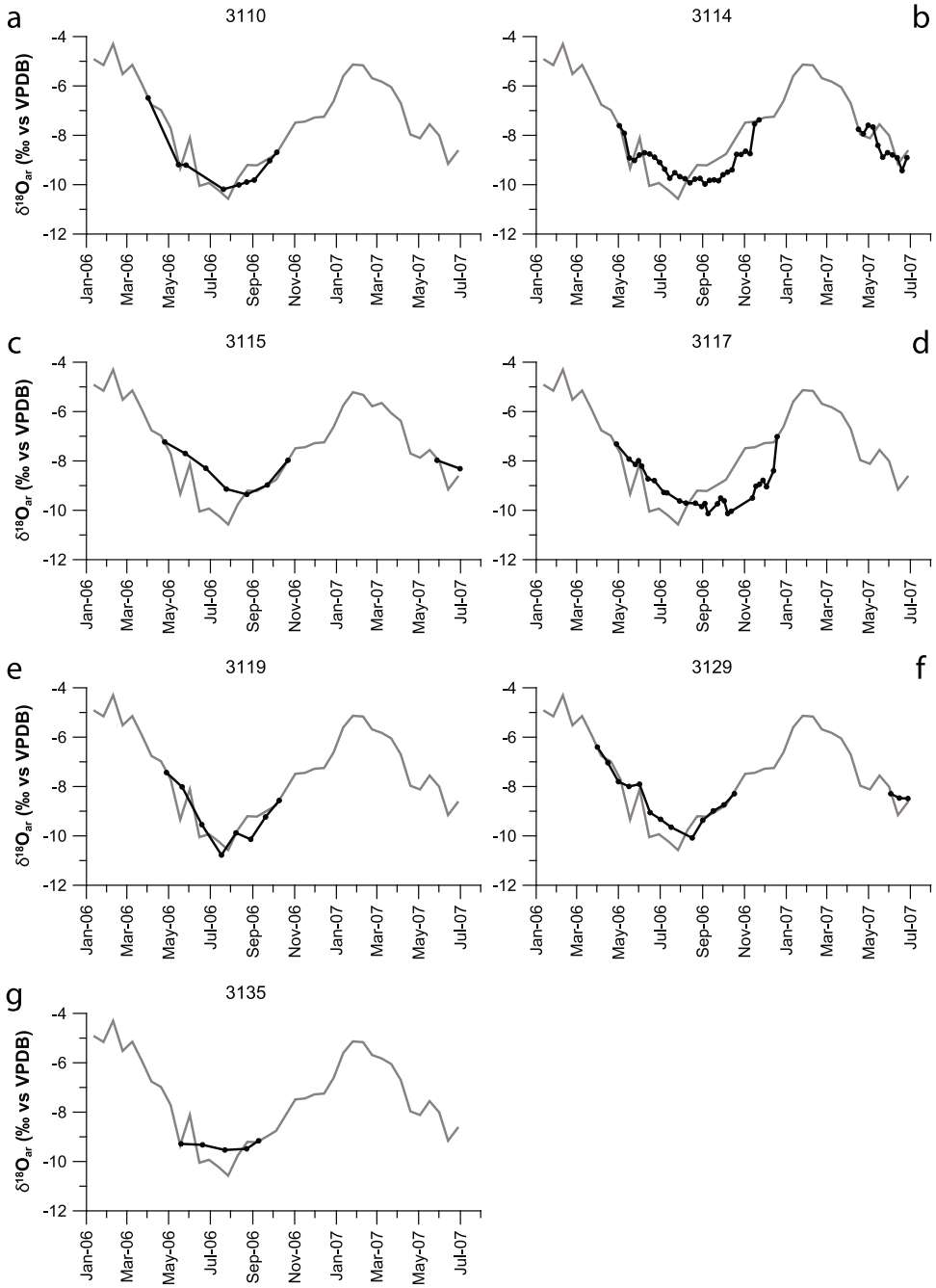

Figure 7. Predicted $\delta^{18}O_{ar}$ values (gray lines) plotted with individual shell $\delta^{18}O_{ar}$ values (solid black lines and symbols) for Hagestein, using a linear growth model.

Hagestein and three shells from Lith (Figure 5g), both amplitude and values of $\delta^{13}C_{ar}$ for the other Hagestein shells correspond well with measured $\delta^{13}C_{HCO3-}$ (Figures 5a–5f).

4.5. Seasonally Resolved Growth Models

[38] The pattern of growth in unionids, like many bivalves, is recorded in the layering in the shell.

Table 2. Predicted and Measured $\delta^{18}O_{ar}$ Values for Ventral Margin Samples

	$\delta^{18}O_w$	T (°C)	Predicted $\delta^{18}O_{ar}$	Measured $\delta^{18}O_{ar}$
3114	−8.60	20.5	−8.64	−8.90
3115	−8.60	20.5	−8.64	−8.32
3129	−8.60	20.5	−8.64	−8.49

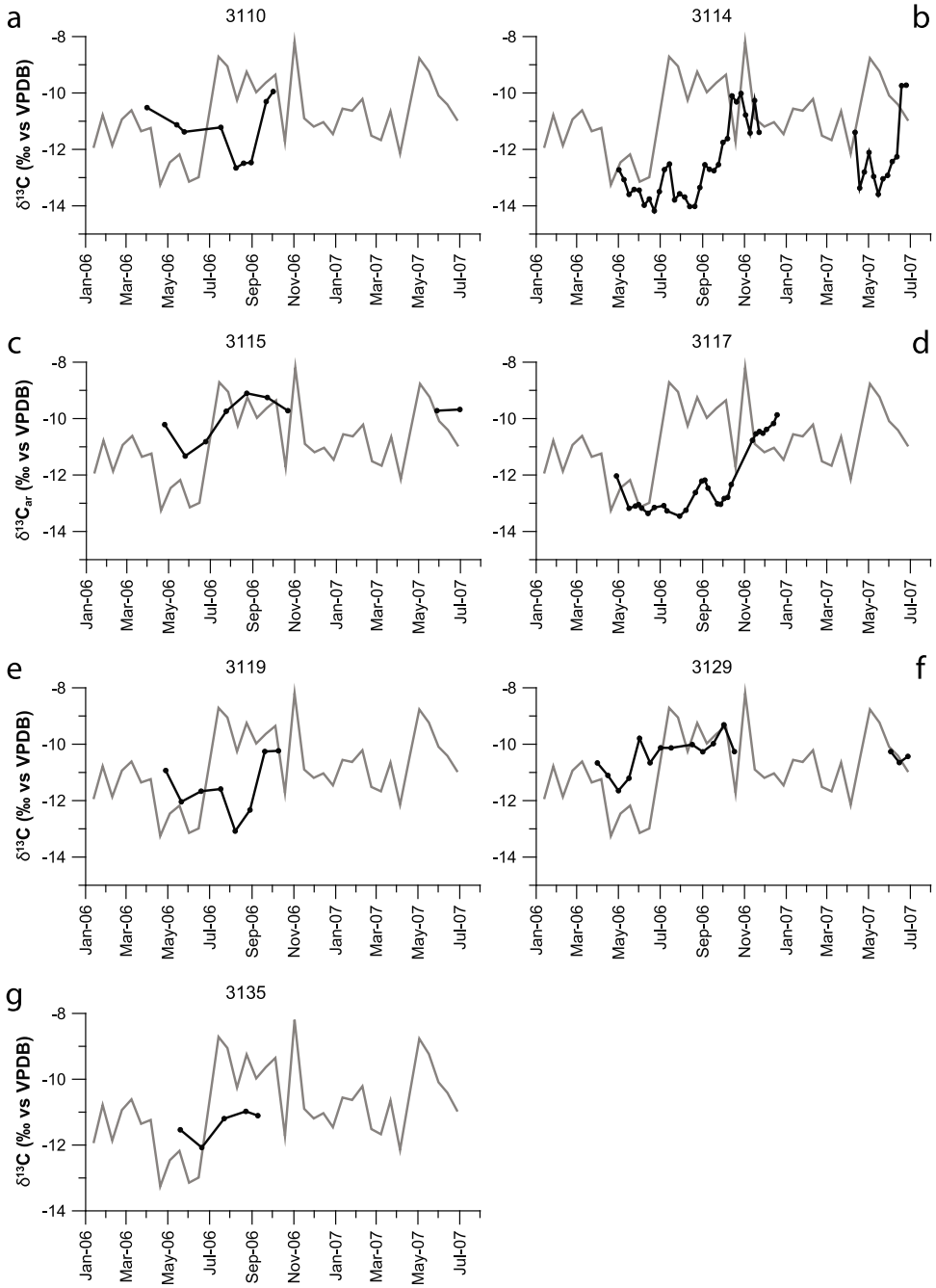

Figure 8. The $\delta^{13}C_{HCO3-}$ values of the Lek river water (gray lines) and $\delta^{13}C_{ar}$ values of each individual shell (solid black lines and symbols).

Discreet growth increments across the transverse sections of the shell are bracketed by distinct lines, commonly referred to as growth lines, representative of the cessation of growth (Figure 4). The origin of these growth lines is commonly inferred to represent the annual growth cessation during winter, but this is often unclear [*Versteegh et al.*, 2009]. For instance, while the onset of the experiment can be clearly be seen as a disturbance line in shell 3114 (caused by handling and/or staining with calcein; Figure 4), the presence of multiple subannual growth lines makes it difficult to locate the winter growth line. These secondary growth lines have been attributed to different factors including predative disturbance and daily periodicity. Thus, because internal growth banding cannot (yet) be used to construct annually resolved growth models, we use the seasonally

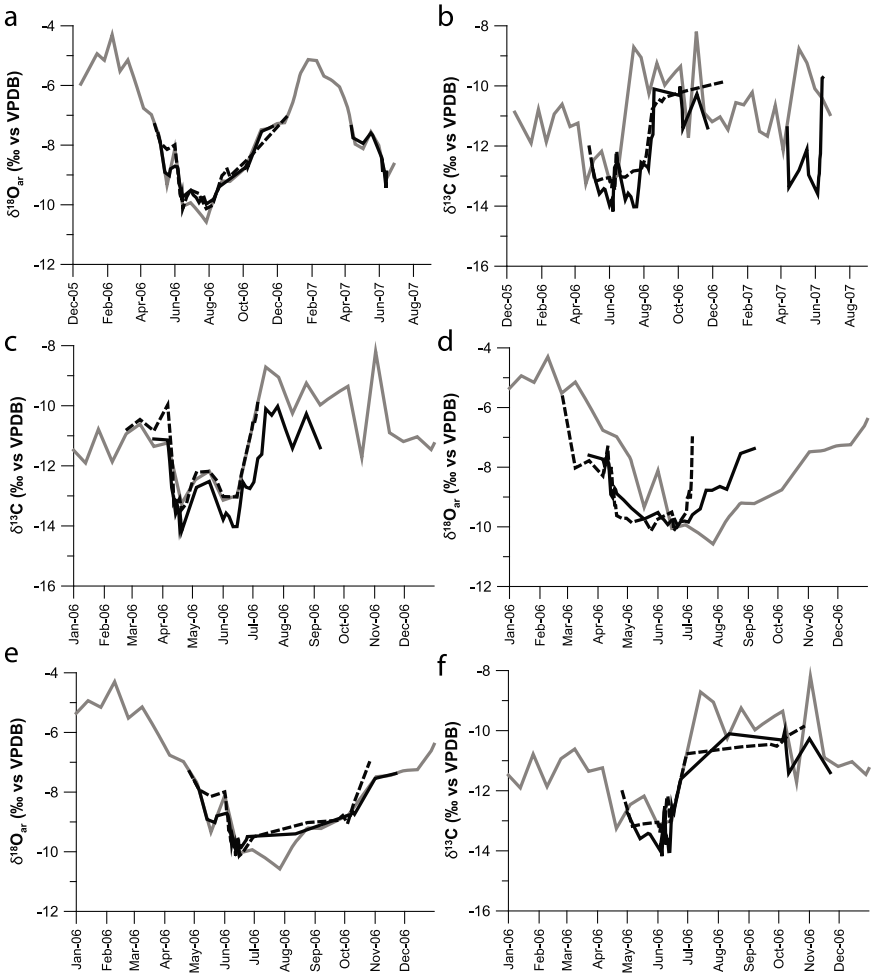

Figure 9. (a) Construction of a growth model using $\delta^{18}O$ values: Shell $\delta^{18}O_{ar}$ records of shells 3114 (solid black line) and 3117 (dashed black line) fitted over the predicted $\delta^{18}O_{ar}$ record (solid gray line) by first matching peaks and troughs and subsequent horizontal shifting of the predicted $\delta^{18}O_{ar}$ record. (b) Shell $\delta^{13}C_{ar}$ records of the same shells plotted with the $\delta^{13}C_{HCO3-}$ record (solid gray line) on the same time axis as Figure 9a. (c) Construction of a growth model using $\delta^{13}C$ values: shell $\delta^{13}C_{ar}$ records of shells 3114 (solid black line) and 3117 (dashed black line) are fitted over the $\delta^{13}C_{HCO3-}$ record (solid gray line) by first matching peaks and troughs and subsequent horizontal shifting of the $\delta^{13}C_{HCO3-}$ record. (d) Shell $\delta^{18}O_{ar}$ records of the same shells plotted over the predicted $\delta^{18}O_{ar}$ record on the same time axis as in Figure 9c. (e) Construction of a growth model using both the $\delta^{18}O$ and the $\delta^{13}C$ records: Shell $\delta^{18}O_{ar}$ records of shells 3114 (solid black line) and 3117 (dashed black line) plotted with the predicted $\delta^{18}O_{ar}$ record (solid gray line). (f) Shell $\delta^{13}C_{ar}$ records of the same shells plotted with the $\delta^{13}C_{HCO3-}$ record (solid gray line) on the same time axis as Figure 9e.

resolved isotopic composition of shells and ambient water.

[39] Given the results of the monitoring experiment both the $\delta^{18}O_{ar}$ and $\delta^{13}C_{ar}$ records appear to record seasonal variation in ambient water. These data sets, combined with the river water $\delta^{18}C_w$ and $\delta^{13}C_{HCO3-}$ records, will now be applied to document variability in intraannual growth rates. We present four seasonally resolved growth models: (1) a linear model; (2) a model based upon predicted and observed seasonal $\delta^{18}O_{ar}$ records; (3) a model based upon the comparison of seasonal $\delta^{13}C_{HCO3-}$ and $\delta^{13}C_{ar}$ records, and (4) a model combining predicted and observed $\delta^{18}O_{ar}$ records as well as $\delta^{13}C_{HCO3-}$ and $\delta^{13}C_{ar}$ records. Construction of these growth models was based upon two specimens of *Unio pictorum* exhibiting the highest growth rates: shells 3114 and 3117.

4.5.1. Model 1: Linear Growth Model

[40] Although it is unlikely that intraannual summer growth is linear, no robust nonlinear growth model is yet available for unionids. Thus, as a first step toward comparison of the measured and predicted

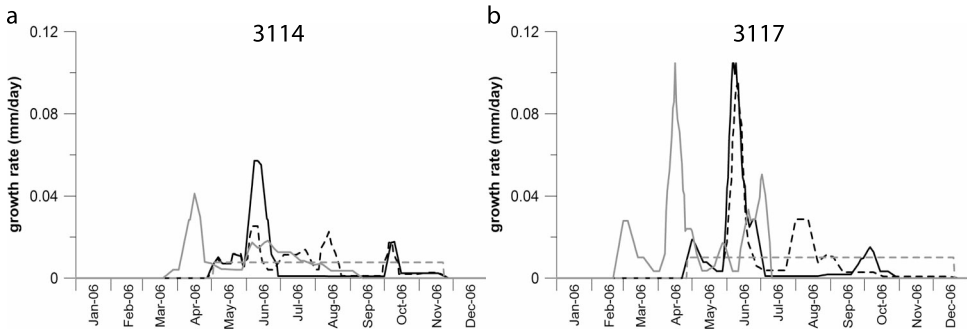

Figure 10. Growth rates of *Unio pictorum* at Hagestein during the growing season. (a) Shell 3114 and (b) shell 3117. For each shell all four growth models are shown. Dashed gray line is the linear model; dashed black line is the δ^{18}O-based model; solid gray line is the δ^{13}C-based model; solid black line is the combined δ^{18}O and δ^{13}C model.

$\delta^{18}O_{ar}$ records and subsequent construction of a seasonally resolved growth model, we assumed linear growth between the previously determined spring and autumn dates of onset and cessation of growth (Figures 7a–7g). A relatively close correspondence between the predicted and measured $\delta^{18}O_{ar}$ records is observed in most shells. However, several growth increment $\delta^{18}O_{ar}$ values are somewhat offset in time compared to predicted values, suggesting a higher growth rate in spring than later in the season (e.g., shells 3114, 3117 and 3129; Figures 7b, 7d, and 7f).

[41] Subsequently, $\delta^{13}C_{HCO3-}$ and shell $\delta^{13}C_{ar}$ values of all Hagestein shells have been plotted using growth rates on the same linear scale as those from the previously discussed $\delta^{18}O_{ar}$ records (Figures 8a–8g). The shapes of the $\delta^{13}C_{HCO3-}$ and $\delta^{13}C_{ar}$ records, plotted using the linear growth rate method, are very similar for five of the shells (i.e., shells 3110, 3114, 3117, 3119 and shell 3115 only in the 2007 season; Figures 8a–8e). However, an offset of about 3 months is apparent between the peaks and troughs of the $\delta^{13}C_{HCO3-}$ and $\delta^{13}C_{ar}$ records. There is no obvious physiological mechanism in these organisms to explain this discrepancy, therefore it is likely an artifact of imposing linearity on seasonally resolved growth.

4.5.2. Model 2: δ^{18}O Peak Matching and Time-Axis Shifting

[42] In order to resolve the environmental factors driving variability in the seasonal growth rate and to reduce the discrepancy between shell and water isotopic data in the linear growth model, a second model based upon peak matching and time-axis shifting of the $\delta^{18}O_{ar}$ data points was constructed (Figure 9a). This results in a growth model with fast growth in early summer and slower growth during the rest of the season. In order to validate this model $\delta^{13}C_{HCO3-}$ and $\delta^{13}C_{ar}$ values were plotted together on the same time-scale (Figure 9b), this reduces the apparent time discrepancy by one third in comparison with the linear model.

4.5.3. Model 3: δ^{13}C Peak Matching and Time-Axis Shifting

[43] Unlike the predicted $\delta^{18}O_{ar}$ record, the $\delta^{13}C_{HCO3-}$ record exhibits several sudden leaps in values; these may serve as tie-points for the model. In this approach, first $\delta^{13}C_{ar}$ records were fitted to the $\delta^{13}C_{HCO3-}$ record using a similar methodology to model 2 (Figures 9c–9d). The model was then compared to predicted and observed $\delta^{18}O_{ar}$ values plotted on the same timescale. In model 3, the time lag between predicted and measured $\delta^{18}O_{ar}$ is in the order of two months, which is similar to the $\delta^{13}C$ time lag in model 2. Hence, there does not appear to be a significant improvement of the growth model when using model 3 as opposed to model 2; what is gained in the better match of $\delta^{13}C$ data is lost in the poorer match of $\delta^{18}O$ data.

4.5.4. Model 4: Combined δ^{18}O and δ^{13}C Records, Peak Matching, and Time-Axis Shifting

[44] Both the $\delta^{18}O_{ar}$ and the $\delta^{13}C_{ar}$ shell profiles appear to record seasonal variation in ambient water of $\delta^{18}O_w$ and $\delta^{13}C_{HCO3-}$, respectively. Therefore, a model simultaneously matching peaks and troughs in the $\delta^{13}C$ and $\delta^{18}O$ records was constructed. This leads to a good match between the predicted and measured $\delta^{18}O_{ar}$ records, as well as the $\delta^{13}C_{ar}$ and $\delta^{13}C_{HCO3-}$ records, if faster growth in early summer is allowed for (Figures 9e, 9f, and 10). As such, growth model 4 appears to resolve time lag discrepancies observed in models 1, 2 and 3.

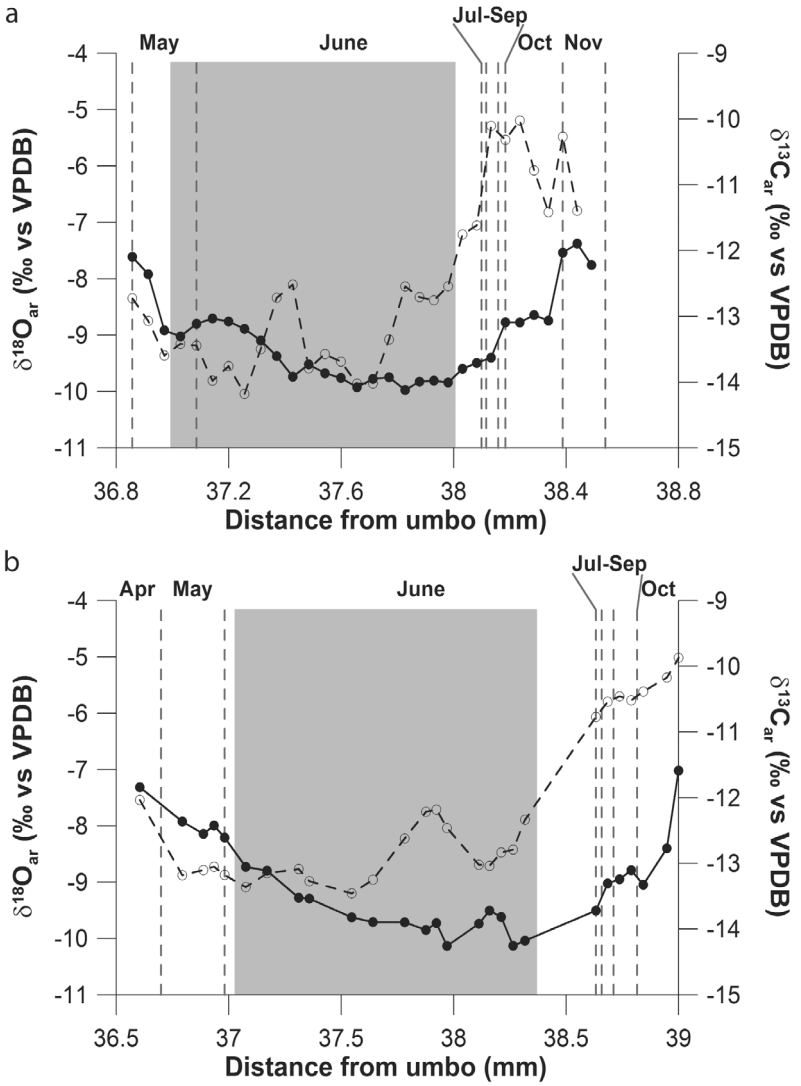

Figure 11. The $\delta^{18}O_{ar}$ and $\delta^{13}C_{ar}$ records of shells (a) 3114 and (b) 3117 with the months during which specific parts of the shell grew indicated. Grey rectangles indicate the episode of fast growth in June.

[45] The approximate 1 month episode of fast growth suggested in growth model 4 is recorded in both shell $\delta^{18}O_{ar}$ and $\delta^{13}C_{ar}$ represented by a broad trough, during which $\delta^{18}O_{ar}$ and $\delta^{13}C$ values remain relatively constant. Months of little or no growth are represented by only a narrow portion of the shell (Figure 11).

4.6. Comparison of the Growth Functions

[46] Growth functions resulting from the four different models are shown in Figures 10a and 10b. Model 1 (linear) obviously has constant growth rates throughout the season. Model 2 ($\delta^{18}O$-based) shows differential growth with three (shell 3114) or two (shell 3117) peaks and low-growth intervals in between. The above-described two-month time shift is evident again when model 3 ($\delta^{13}C$-based) is compared to the model 2. Model 4 (combined $\delta^{18}O$/$\delta^{13}C$) shows a large growth peak at the same time as model 2, followed by a time interval of low growth and then a smaller peak before growth ceases during winter (Figures 10a and 10b). This model provides the best fit, because it aligns shifts in both $\delta^{18}O$ and $\delta^{13}C$ records. As such, model 4 supposedly yields the most accurate representation of intraannual growth (Figure 10).

[47] In summary, these species of *Unio* start growing when water temperatures reach 13.5°C in spring. Growth continues at a moderate rate during spring, before accelerating to up to five times the previous

growth rate during early summer (June), potentially representing an abundance of food. As time progresses growth slows down considerably, until it comes to a complete halt when temperatures fall below 13.5°C again. The growth peak in June coincides with the chlorophyll *a* peak in the river, suggesting that, intraannual growth is mainly influenced by phytoplankton abundance (Figure 3a; chlorophyll *a*). This factor was already known to have a positive effect on the ontogenetic growth of North-American Unionidae [*Kesler et al.*, 2007] and European *Anodonta* [*Jokela and Mutikainen*, 1995], although unionids feed on bacteria and fine particulate organic matter as well [*Christian et al.*, 2004; *Nichols and Garling*, 2000; *Vaughn and Hakenkamp*, 2001]. It has to be noted that other factors influencing growth cannot be entirely ruled out. These might include pollution with heavy metals, low oxygen content of the water and elevated salinities, especially in dry time intervals [*Admiraal et al.*, 1993; *Hartmann et al.*, 2007].

[48] The water $\delta^{13}C_{HCO3-}$ record exhibits significant differences between samples taken every fortnight and clearly has not enough time-resolution to reveal all high frequency variation. Higher time-resolution sampling could possibly have enabled a more precise fit of both the $\delta^{18}O_{ar}$ and $\delta^{13}C_{ar}$ records to the predicted $\delta^{18}O_{ar}$ and ambient water $\delta^{13}C_{HCO3-}$ record.

5. Conclusions

[49] We have demonstrated that unionid species, living in the Rhine and Meuse rivers, precipitate skeletal aragonite in oxygen isotopic equilibrium with ambient water. Shell $\delta^{18}O_{ar}$ values are a result of ambient water $\delta^{18}O_w$ values and temperature. River $\delta^{13}C_{HCO3-}$ values exhibit a seasonal cycle with low values in winter and spring. Suddenly rising values in early summer are due to preferential removal of ^{12}C from the DIC pool by phytoplankton photosynthesis. This seasonal $\delta^{13}C_{HCO3-}$ cycle is accurately recorded in $\delta^{13}C_{ar}$ values of growth increments in unionid shells.

[50] Based on a correlation of intraannual $\delta^{18}O$ and $\delta^{13}C$ variation in ambient water and shells, a growth model was constructed which indicates nonlinear growth of these unionids. These data suggest that onset and cessation of growth of unionid freshwater mussels are dependent on water temperature, while the rate of growth is dependent on primary productivity (food availability).

[51] This study demonstrates the potential of unionid shell chemistry for palaeoclimate studies. Freshwater bivalve $\delta^{18}O_{ar}$ records can serve as a proxy for past river $\delta^{18}O_w$ values, in relation to discharge seasonality and river dynamics. Freshwater bivalve records can potentially serve as a proxy for past primary productivity, although other parameters (e.g., CO_2 exchange with atmosphere) will likely affect $\delta^{13}C_{ar}$ as well.

Acknowledgments

[52] This project was financed by BSIK - Climate changes Spatial Planning. We are greatly indebted to Piet Versteegh and Marie-Louise Friedrichs for their help with water sampling. Furthermore we would like to thank Willem Mook, Rijkswaterstaat (Dutch Directorate for Public Works and Water Management) and the Centre for Isotope Research (University of Groningen) for providing data sets. The constructive comments of Elena Dunca and an anonymous reviewer greatly improved the quality of this paper. This is NSG publication 20090101.

References

Admiraal, W., et al. (1993), The rivers Rhine and Meuse in the Netherlands: Present state and signs of ecological recovery, *Hydrobiologia*, *265*(1), 97–128.

Al-Aasm, I. S., et al. (1998), Stable isotopes and heavy metal distribution in *Dreissena polymorpha* (zebra mussels) from western basin of Lake Erie, *Canada, Environ. Geol.*, *33*(2–3), 122–129, doi:10.1007/s002540050232.

Anthony, J. L., et al. (2001), Length-specific growth rates in freshwater mussels (Bivalvia: Unionidae): Extreme longevity or generalized growth cessation?, *Freshwater Biol.*, *46*(10), 1349–1359, doi:10.1046/j.1365-2427.2001.00755.x.

Arter, H. E. (1989), Effect of eutrophication on species composition and growth of freshwater mussels (Mollusca, Unionidae) in Lake Hallwil (Aargau, Switzerland), *Aq. Sci. Res. Across Boundaries*, *51*(2), 87–99.

Aucour, A.-M., et al. (2003), $\delta^{13}C$ of fluvial mollusk shells (Rhône River): A proxy for dissolved inorganic carbon?, *Limnol. Oceanogr.*, *48*(6), 2186–2193, doi:10.4319/lo.2003.48.6.2186.

Buhl, D., et al. (1991), Nature and nurture: Environmental isotope story of the River Rhine, *Naturwissenschaften*, *78*(8), 337–346, doi:10.1007/BF01131605.

Christian, A. D., et al. (2004), Trophic position and potential food sources of 2 species of unionid bivalves (Mollusca: Unionidae) in 2 small Ohio streams, *J. North Am. Benthol. Soc.*, *23*(1), 101–113, doi:10.1899/0887-3593(2004)023<0101:TPAPFS>2.0.CO;2.

Clark, G. R., II (2005), Daily growth lines in some living Pectens (Mollusca: Bivalvia), and some applications in a fossil relative: Time and tide will tell, *Palaeogeogr. Palaeoclimatol. Palaeoecol.*, *228*(1–2), 26–42, doi:10.1016/j.palaeo.2005.03.044.

Clark, I. D., and P. Fritz (1997), *Environmental Isotopes in Hydrogeology*, 1st ed., 328 pp., Lewis, New York.

Dettman, D. L., et al. (1999), Controls on the stable isotope composition of seasonal growth bands in aragonitic freshwater bivalves (Unionidae), *Geochim. Cosmochim. Acta*, *63*(7–8), 1049–1057, doi:10.1016/S0016-7037(99)00020-4.

Dunca, E., and H. Mutvei (2001), Comparison of microgrowth pattern in *Margaritifera margaritifera* shells from south and north Sweden, *Am. Malacol. Bull.*, *16*(1–2), 239–250.

Dunca, E., et al. (2005), Freshwater bivalves tell of past climates: But how clearly do shells from polluted rivers speak?, *Palaeogeogr. Palaeoclimatol. Palaeoecol.*, *228*(1–2), 43–57, doi:10.1016/j.palaeo.2005.03.050.

Fastovsky, D. E., et al. (1993), Freshwater bivalves (Unionidae), disequilibrium isotopic fractionation, and temperatures, *Palaios*, *8*(6), 602–608, doi:10.2307/3515035.

Freitas, P. S., et al. (2006), Environmental and biological controls on elemental (Mg/Ca, Sr/Ca and Mn/Ca) ratios in shells of the king scallop *Pecten maximus*, *Geochim. Cosmochim. Acta*, *70*(20), 5119–5133, doi:10.1016/j.gca.2006.07.029.

Fritz, P., and S. Poplawski (1974), ^{18}O and ^{13}C in the shells of freshwater molluscs and their environments, *Earth Planet. Sci. Lett.*, *24*(1), 91–98, doi:10.1016/0012-821X(74)90012-0.

Gajurel, A. P., et al. (2006), C and O isotope compositions of modern fresh-water mollusc shells and river waters from the Himalaya and Ganga plain, *Chem. Geol.*, *233*(1–2), 156–183, doi:10.1016/j.chemgeo.2006.03.002.

Geist, J., et al. (2005), Stable carbon isotopes in freshwater mussel shells: Environmental record or marker for metabolic activity?, *Geochim. Cosmochim. Acta*, *69*(14), 3545–3554, doi:10.1016/j.gca.2005.03.010.

Gillikin, D. P., et al. (2006), Stable carbon isotopic composition of *Mytilus edulis* shells: Relation to metabolism, salinity, $\delta^{13}C_{DIC}$ and phytoplankton, *Org. Geochem.*, *37*(10), 1371–1382, doi:10.1016/j.orggeochem.2006.03.008.

Gillikin, D. P., et al. (2009), Ontogenic increase of metabolic carbon in freshwater mussel shells (*Pyganodon cataracta*), *J. Geophys. Res.*, *114*, G01007, doi:10.1029/2008JG000829.

Gittenberger, E., et al. (1998), *De Nederlandse zoetwatermollusken - Recente en fossiele weekdieren uit zoet en brak water*, 1st ed., 288 pp., Natl. Natuurhist. Mus. Naturalis, Leiden, Netherlands.

Goewert, A., et al. (2007), Oxygen and carbon isotope ratios of *Lampsilis cardium* (Unionidae) from two streams in agricultural watersheds of Iowa, USA, *Palaeogeogr. Palaeoclimatol. Palaeoecol.*, *252*(3–4), 637–648, doi:10.1016/j.palaeo.2007.06.002.

Gonfiantini, R., et al. (1995), Standards and intercomparison materials distributed by the International Atomic Energy Agency for stable isotope measurements, pp. 13–29, Int. At. Energy Agency, Vienna.

Goodwin, D. H., et al. (2003), Resolution and fidelity of oxygen isotopes as paleotemperature proxies in bivalve mollusk shells: Models and observations, *Palaios*, *18*(2), 110–125, doi:10.1669/0883-1351(2003)18<110:RAFOOI>2.0.CO;2.

Grossman, E. L., and T.-L. Ku (1986), Oxygen and carbon isotope fractionation in biogenic aragonite: Temperature effects, *Chem. Geol.*, *59*, 59–74, doi:10.1016/0168-9622(86)90057-6.

Hartmann, J., et al. (2007), Geochemistry of the river Rhine and the upper Danube: Recent trends and lithological influence on baselines, *J. Environ. Sci. Sustainable Soc.*, *1*, 39–46, doi:10.3107/jesss.1.39.

Howard, A. D. (1922), Experiments in the culture of freshwater mussels, *Bull. Bur. Fish.*, *38*, 63–89.

Jokela, J., and P. Mutikainen (1995), Phenotypic plasticity and priority rules for energy allocation in a freshwater clam: A field experiment, *Oecologia*, *104*(1), 122–132, doi:10.1007/BF00365570.

Kaandorp, R. J. G., et al. (2003), Seasonal stable isotope variations of the modern Amazonian freshwater bivalve *Anodontites trapesialis*, *Palaeogeogr. Palaeoclimatol. Palaeoecol.*, *194*(4), 339–354, doi:10.1016/S0031-0182(03)00332-8.

Kesler, D. H., et al. (2007), Long-term monitoring of growth in the Eastern Elliptio, *Elliptio complanata* (Bivalvia: Unionidae), in Rhode Island: A transplant experiment, *J. North Am. Benthol. Soc.*, *26*(1), 123–133, doi:10.1899/0887-3593(2007)26[123:LMOGIT]2.0.CO;2.

Lemarié, D. P., et al. (2000), Evaluation of tag types and adhesives for marking freshwater mussels (Mollusca: Unionidae), *J. Shellfish Res.*, *19*(1), 247–250.

McConnaughey, T. A., and D. Gillikin (2008), Carbon isotopes in mollusk shell carbonates, *Geo Mar. Lett.*, *28*(5–6), 287–299, doi:10.1007/s00367-008-0116-4.

McConnaughey, T. A., et al. (1997), Carbon isotopes in biological carbonates: Respiration and photosynthesis, *Geochim. Cosmochim. Acta*, *61*(3), 611–622, doi:10.1016/S0016-7037(96)00361-4.

Mook, W. G. (1968), Geochemistry of the stable carbon and oxygen isotopes of natural waters in the Netherlands, Ph.D. thesis, 157 pp., Univ. of Groningen, Groningen, Netherlands.

Mook, W. G. (2000), *Environmental Isotopes in the Hydrological Cycle: Principles and Applications*, vol. 1, *Introduction, Theory, Methods and Reviews, 280 pp., Int. At. Energy Agency, Vienna.*

Mook, W. G., and J. C. Vogel (1968), Isotopic equilibrium between shells and their environment, *Science*, *159*(3817), 874–875, doi:10.1126/science.159.3817.874.

Morris, T. J., and L. D. Corkum (1999), Unionid growth patterns in rivers of differing riparian vegetation, *Freshwater Biol.*, *42*(1), 59–68, doi:10.1046/j.1365-2427.1999.00468.x.

Negus, C. L. (1966), A quantitative study of growth and production of unionid mussels in the river Thames at Reading, *J. Anim. Ecol.*, *35*(3), 513–532, doi:10.2307/2489.

Nichols, S. J., and D. Garling (2000), Food-web dynamics and trophic-level interactions in a multispecies community of freshwater unionids, *Can. J. Zool.*, *78*(5), 871–882, doi:10.1139/cjz-78-5-871.

Raikow, D. F., and S. K. Hamilton (2001), Bivalve diets in a Midwestern U.S. stream: A stable isotope enrichment study, *Limnol. Oceanogr.*, *46*(3), 514–522, doi:10.4319/lo.2001.46.3.0514.

Ricken, W., et al. (2003), Recent and historical discharge of a large European river system—Oxygen isotopic composition of river water and skeletal aragonite of Unionidae in the Rhine, *Palaeogeogr. Palaeoclimatol. Palaeoecol.*, *193*(1), 73–86, doi:10.1016/S0031-0182(02)00713-7.

Romanek, C. S., et al. (1992), Carbon isotopic fractionation in synthetic aragonite and calcite: Effects of temperature and precipitation rate, *Geochim. Cosmochim. Acta*, *56*(1), 419–430, doi:10.1016/0016-7037(92)90142-6.

Ross, K. A., et al. (2001), An assessment of some methods for tagging the great scallop, *Pecten maximus*, *J. Mar. Biol. Assoc. U. K.*, *81*(6), 975–977.

Valdovinos, C., and P. Pedreros (2007), Geographic variations in shell growth rates of the mussel *Diplodon chilensis* from temperate lakes of Chile: Implications for biodiversity conservation, *Limnologica*, *37*(1), 63–75.

Vaughn, C. C., and C. C. Hakenkamp (2001), The functional role of burrowing bivalves in freshwater ecosystems, *Freshwater Biol.*, *46*(11), 1431–1446, doi:10.1046/j.1365-2427.2001.00771.x.

Veinott, G. I., and R. J. Cornett (1998), Carbon isotopic disequilibrium in the shell of the freshwater mussel *Elliptio complanata*, *Appl. Geochem.*, *13*(1), 49–57, doi:10.1016/S0883-2927(97)00053-X.

Verdegaal, S., et al. (2005), Stable isotopic records in unionid shells as a paleoenvironmental tool, *Neth. J. Geosci.*, *84*(4), 403–408.

Versteegh, E. A. A. (2009), Silent witnesses—Freshwater bivalves as archives of environmental variability in the Rhine-Meuse delta, Ph.D. thesis, 208 pp., VU Univ., Amsterdam.

Versteegh, E. A. A., et al. (2009), Oxygen isotopic composition of bivalve seasonal growth increments and ambient water in the rivers Rhine and Meuse, *Palaios*, *24*(8), 497–504, doi:10.2110/palo.2008.p08-071r.

Versteegh, E. A. A., et al. (2010), Can shells of freshwater mussels (Unionidae) be used to estimate low summer discharge of rivers and associated droughts?, *Int. J. Earth Sci.*, doi:10.1007/s00531-010-0551-0, in press.

Zeebe, R. E., and D. Wolf-Gladrow (2001), *CO_2 in Seawater: Equilibrium, Kinetics, Isotopes*, 1st ed., 346 pp., Elsevier, Amsterdam.